Impact of model resolution on the representation of deep water formation and its link with the AMOC

Eneko Martin-Martinez[1,2], **Eduardo Moreno-Chamarro**[1], **Pablo Ortega**[1], **Amanda Frigola**[1], **Bernat Jiménez-Esteve**[1], **Daria Kuznetsova**[1], **Aude Carréric**[1], **Saskia Loosveldt-Tomas**[1], **Pierre-Antoine Bretonnière**[1], **Margarida Samsó Cabré**[1]

1: Barcelona Supercomputing Center (BSC) 2: Departament de Dinàmica de la Terra i l'Oceà, Facultat de Ciències de la Terra, Universitat de Barcelona (UB)

Preliminary results

- Mixing region is shifted to Labrador Sea when increasing the model resolution
- Surface wind-stress is the main mixing driver
- *EC-Earth3P-VHR* shows no propagation of the mixing imprint in the *MOC* to lower latitudes

Methods

- 1950-control experiments
- HighResMIP protocol
- 76 years (removed the first 30 years with model drift)
- 95 % of confidence (non-significant regions masked).

Discussion

- First PC of *sigma2* profile is related to the first *MLD* series, around 0.95 correlation coefficient in all the cases
- Positive/negative NAO induced wind-stress enhances/diminishes the mixing in the *EC-Earth3P-VHR* and *EC-Earth3P-HR* models
- Influence of westward propagated salinity anomalies in *EC-Earth3P-VHR*
- Propagation downward and southward of the density anomalies forced by deep-water mixing
- Different responses on the AMOC to the deep-water-mixing: *EC-Earth3P* shows a deeper propagation which arrives to low latitudes, *EC-Earth3P-HR* shows propagation to middle latitudes, *EC-Earth3P-VHR* shows only local changes

Ongoing and future analyses

- Continue exploring the impacts of deep-water mixing in the three different resolutions
- Study the impact of Greenland land-ice melting in the deep-water mixing and the MOC
- Explore other climate impacts related to the mesoescale processes and deep-water mixing

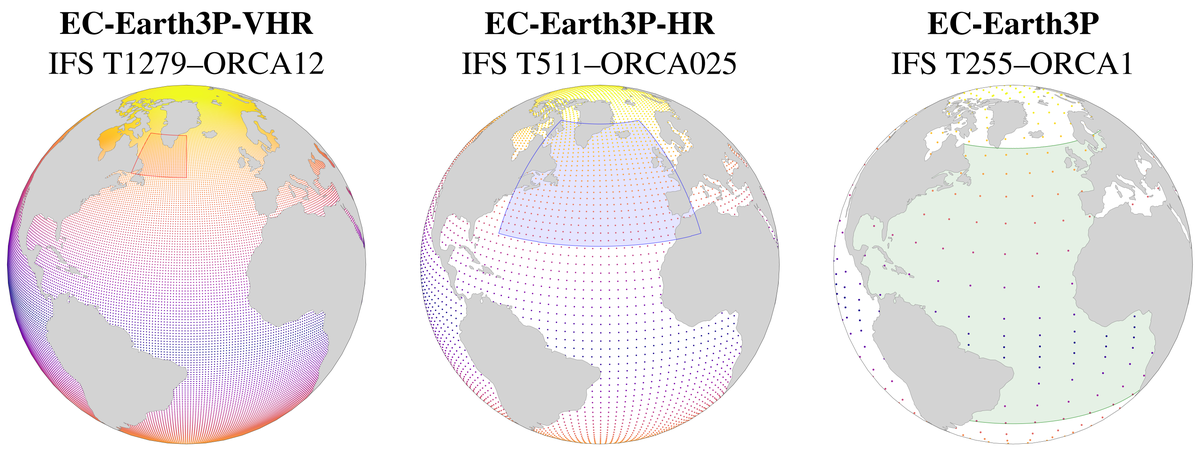

Figure 1: Representation of the ORCA grids used in the EC-Earth3P configurations. Each dot represents 10x10 grid points. Each figure shows one of the regions we have used: subpolar gyre box (left, red box), North Atlantic box (middle, blue box), and Atlantic basin (right, green area).

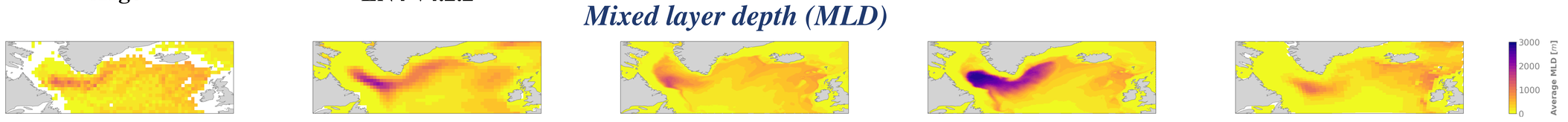

Figure 2: *MLD* time-average.

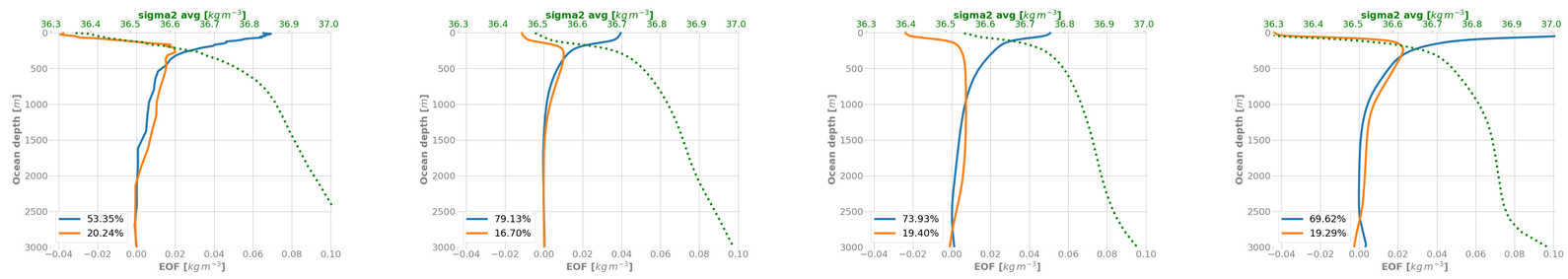

Figure 3: First and second EOFs of density profiles for *sigma2* average in the subpolar gyre box (see Figure 1).

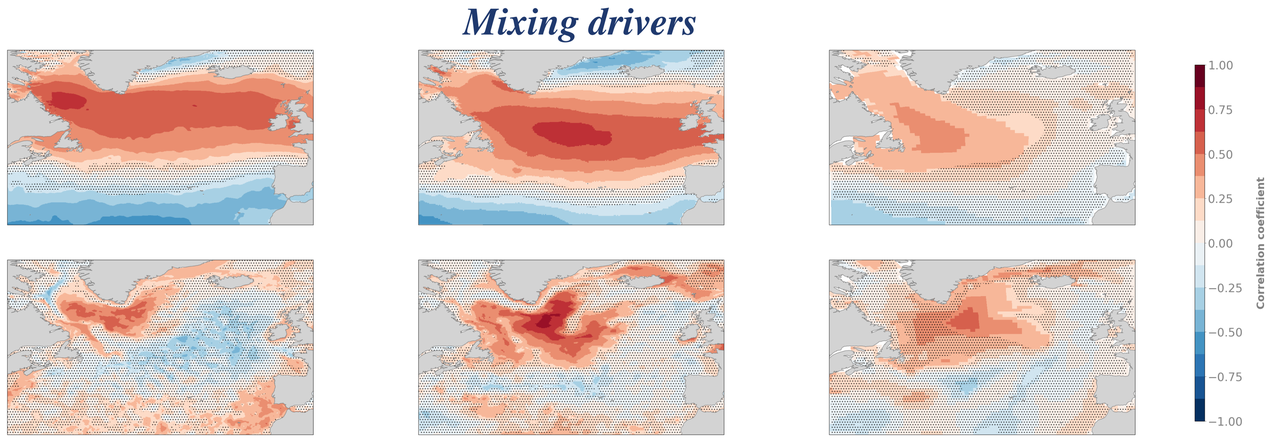

Figure 4: Correlation of the *MLD* average in the subpolar gyre box (see Figure 1) with τ_x (top row) and *SSS* (bottom row).

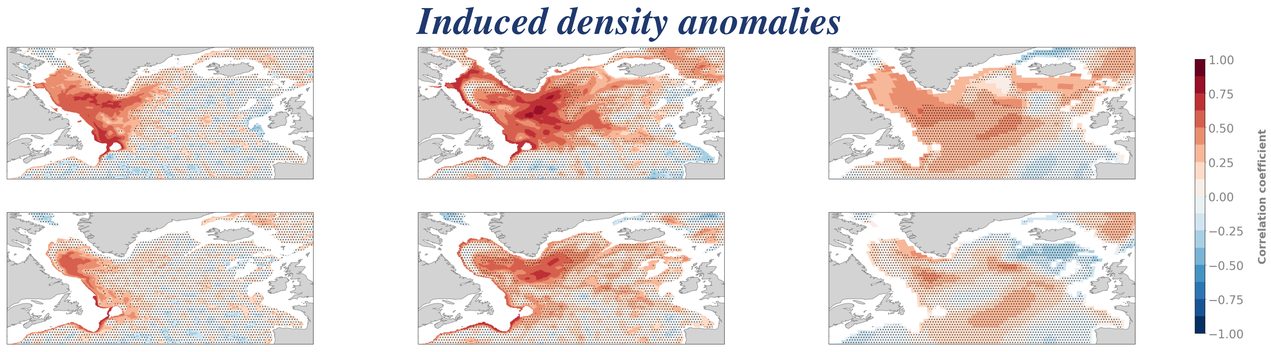

Figure 5: Correlation of the *MLD* average in the subpolar gyre box (see Figure 1) with *sigma2* lagged one year at $500\,m$ (top row) and $1000\,m$ (bottom row).

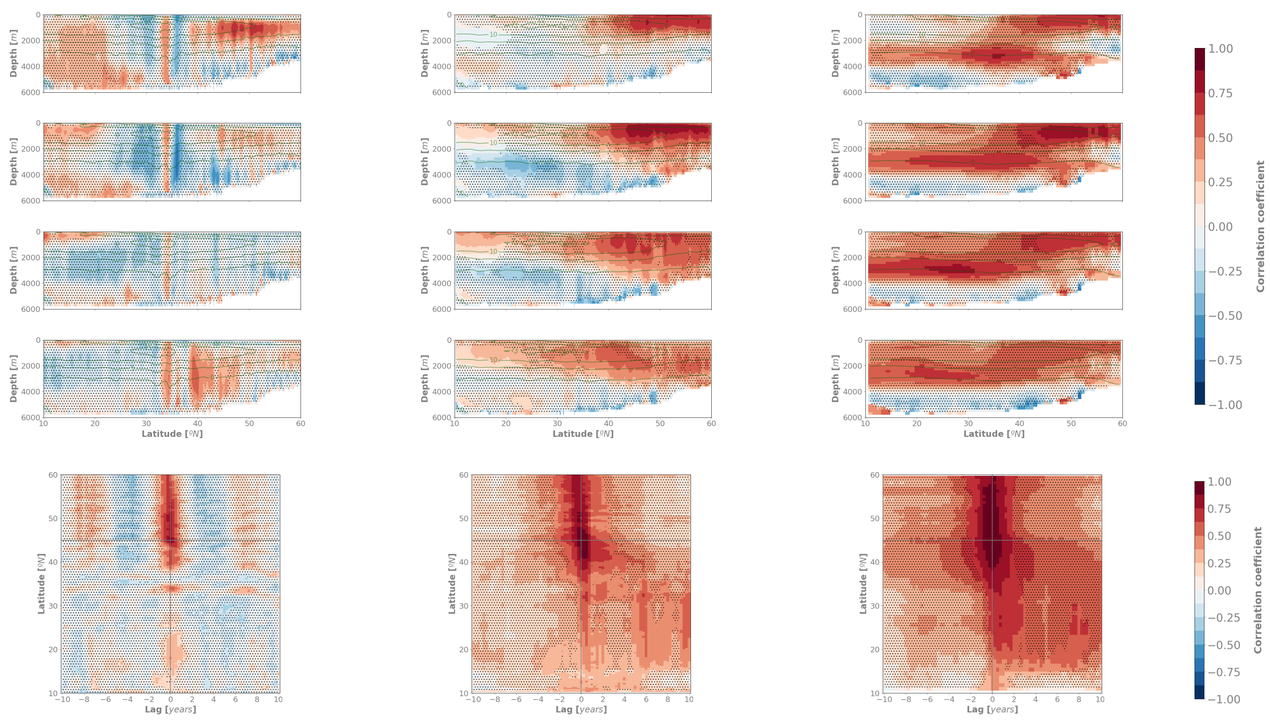

Figure 6: Correlation of the 3-year low-pass filtered *MLD* average in the subpolar gyre box (see Figure 1) with 3-year low-pass filtered and lagged *MOC* removing the Ekman transport in the Atlantic basin (see Figure 1). No-lag (top row) and lags of two years, four years, six years with the *MOC* lagging (second row, third row, bottom row).

Figure 7: Correlation of the yearly *maxMOC* without the Ekman transport at 45º with the yearly *maxMOC* without the Ekman transport from 10ºN to 60ºN.

Scan and share

Contact

eneko.martin@bsc.es

linkedin.com/in/eneko-martin

Barcelona Supercomputing Center
Centro Nacional de Supercomputación

EERIE European Eddy-Rich ESMs

STREAM

Grant *PRE2021-097163* funded by:

MINISTERIO DE CIENCIA E INNOVACIÓN

UNIÓN EUROPEA
Fondo Social Europeo
El FSE invierte en tu futuro

AGENCIA ESTATAL DE INVESTIGACIÓN